Computer Networks 216 (2022) 109252

Contents lists available at ScienceDirect

Computer Networks

journal homepage: www.elsevier.com/locate/comnet

Enhancing LoRaWAN scalability with Longest First Slotted CSMA

Sergio Herrería-Alonso *, Andrés Suárez-González, Miguel Rodríguez-Pérez, Cándido López-García

atlanTTic Research Center, Universidade de Vigo, 36310 Vigo, Spain

ARTICLE INFO

Keywords:
LPWAN
LoRa
LoRaWAN
Aloha
CSMA

ABSTRACT

Compelling features such as low power consumption and low complexity make LoRaWAN one of the most promising technologies to provide long-range connectivity to resource-constrained devices. However, LoRaWAN suffers from limited scalability since it uses an Aloha-based protocol for accessing the channel that causes a huge amount of frame collisions when the number of devices (or the network load) is high. This paper presents LFS-CSMA, a new medium access control mechanism that enhances the scalability of LoRaWAN networks by just combining the well-known slotted Aloha and CSMA schemes in a novel manner. With LFS-CSMA, longer frames are transmitted earlier within a given timeslot. Thus, devices with short frames to be transmitted can check the channel availability before sending them and avoid collisions if they detect an ongoing transmission. Performance results show that LFS-CSMA causes far less collisions than traditional MAC mechanisms, thus improving the scalability of LoRaWAN networks significantly.

1. Introduction

Throughout the last few years, Internet of Things (IoT) technologies have been attracting increased attention from both industry and research communities since they make possible the connection of huge amounts of resource-constrained devices to the Internet [1]. Emerging IoT networks offer, therefore, the potential to support a wide range of applications including, among others, remote health monitoring, vehicular communications, home automation, emergency notification systems, smart city and industrial monitoring.

One IoT technology that is currently gaining great relevance is Low Power Wide Area Networks (LPWAN). Different from other cellular and short-range wireless technologies, LPWAN provides long-range connectivity for low power and low data rate IoT devices [2]. In particular, LPWAN enables wide area coverage to lots of power-constrained devices that just need to sporadically transmit short messages over long distances. Within LPWAN solutions [3], the most popular technologies are SigFox, NB-IoT, LTE-M, DASH7 and LoRaWAN.

In this paper, we focus on LoRaWAN networks [4]. Promoted by the LoRa Alliance [5], LoRaWAN defines an open protocol stack to operate over the LoRa (Long Range) physical layer on unlicensed bands [6]. The main LoRaWAN features (i.e., long range, low power requirements, low complexity and open specifications) make it one of the most promising LPWAN technologies. However, one of the most critical weak points reported for this technology is its limited scalability [7]. According to the LoRaWAN specifications, most devices follow a simple Aloha-based protocol for accessing the channel, so they just transmit their frames without restraint as long as they have data to send. Certainly, this simple Medium Access Control (MAC) mechanism is suitable for monitoring applications requiring sporadic data transmissions but, as the number of devices (or the network load) increases, it becomes excessively inefficient since it will be more likely that multiple devices transmit at the same time, thus causing lots of collisions. Therefore, large-scale LoRaWAN networks with high traffic load require more efficient MAC schemes.

Many alternative random access MAC mechanisms have been proposed to enhance scalability of LoRaWAN networks [8–14]. They are mostly variants of the well-known slotted Aloha and CSMA (Carrier Sense Multiple Access) schemes. Slotted Aloha splits the channel into discrete timeslots of fixed duration and then forces devices to start their transmissions at the beginning of a timeslot, whereas, with CSMA, devices must check the availability of the channel before sending their frames. There are also some scheduled time-slotted mechanisms that allocate each timeslot to a unique sending device, thus avoiding collisions [15–18]. These contention-free mechanisms could significantly improve efficiency but, unfortunately, they are very difficult to deploy since the coordination of transmissions in LoRaWAN networks is a really challenging task [19].

This paper presents LFS (Longest First Slotted)-CSMA, a new MAC scheme that enhances the scalability of LoRaWAN networks by just

* Corresponding author.
E-mail address: sha@det.uvigo.es (S. Herrería-Alonso).

https://doi.org/10.1016/j.comnet.2022.109252
Received 14 February 2022; Received in revised form 20 June 2022; Accepted 30 July 2022
Available online 9 August 2022

combining both slotted Aloha and CSMA mechanisms in a careful manner. To the best of our knowledge, this is the first time this approach has been investigated for this kind of networks. Unlike slotted Aloha, our proposal allows frames within a given timeslot to be transmitted at different instants. Specifically, LFS-CSMA schedules frame transmissions according to their durations so that longer frames are transmitted earlier in the timeslot. This helps to reduce the amount of collisions, since those devices with short frames to be transmitted have some time to detect the ongoing transmission of a larger frame and reschedule their own transmissions. We also develop an analytical model to evaluate the performance of our scheme and some basic random access mechanisms (pure Aloha, slotted Aloha and non-persistent CSMA). Performance results show that LFS-CSMA clearly outperforms all the classic schemes improving the scalability of LoRa transmissions significantly.

The rest of the paper is organized as follows. In Section 2, we review the main LoRa and LoRaWAN characteristics and discuss some recent MAC schemes proposed for these networks. Then, Section 3 presents the new LFS-CSMA scheme. In Section 4 we develop the analytical model used to evaluate the performance of the MAC schemes. Numerical results are shown in Section 5. Finally, we discuss some relevant deployment issues in Section 6 and summarize the main conclusions in Section 7.

2. Related work

2.1. LoRa

LoRa is a proprietary chirp spread spectrum based modulation technique developed by Semtech for license-free sub-gigahertz radio frequency bands [6]. LoRa performance depends on several configurable radio parameters such as the spreading factor (SF), the channel bandwidth (BW) and the coding rate (CR). LoRa supports multiple SFs, ranging from 7 to 12, to balance the trade-off between coverage range and data rate: increasing the SF permits reaching longer distances, but at the cost of reducing the data rate and consuming more energy.

In addition to the SF, LoRa transceivers can also select the channel bandwidth in the range from 7.8 kHz to 500 kHz, although they typically operate at 125, 250 or 500 kHz. A narrower BW will increase reception sensitivity while the bit rate is reduced. Additionally, LoRa provides multiple orthogonal channels for each given BW to increase network capacity.

LoRa also uses forward error correction (FEC) coding to increase the reception sensitivity and improve protection against interference. Four different coding rates can be used: 4/5, 4/6, 4/7 and 4/8, denoted as CR 1 to CR 4, respectively. More redundant overhead bits are sent with higher CRs, thus increasing resilience against interference at the expense of lowering data bit rate.

LoRa data frames include a preamble, a PHY header, the data payload and the payload CRC resulting of applying the chosen FEC code. The preamble permits synchronizing the receiver with the transmitter. It consists of two parts: a fixed one, comprising 4.25 symbols, and a configurable one that can have a length from 6 up to 65532 symbols (8 symbols by default). The payload size is also configurable, although LoRa limits the PHY message (the frame without considering the preamble) size to a maximum of 255 bytes.

2.2. LoRaWAN

While LoRa defines the lower physical layer, LoRaWAN specifies the MAC protocol and the network architecture to be used with it [4]. In the LoRaWAN architecture, end devices (EDs) communicate with gateways (GWs) forming a star topology. The GWs act as relays forwarding all messages between the EDs and a network server that manages the entire network. LoRaWAN specifies three different types of EDs (classes A, B and C) based on their downlink traffic requirements and energy constraints. In this paper, we focus on Class A, the most popular and energy efficient one. This class is intended for battery-powered nodes with stringent energy constraints. Class A EDs only wake up when they have some data to transmit to the GW. Every uplink transmission can then be optionally followed by one or two receiving windows used for the GW to send acknowledgments or commands in the downlink.

Class A EDs access the channel using a mechanism based on pure Aloha (P-ALOHA). Thus, every time an ED has data to transmit, it sends a frame without using any control mechanism. Despite its simplicity, P-ALOHA provides good enough performance in LoRaWAN networks with low loads: since SFs are quasi-orthogonal[1] and LoRa provides multiple transmission channels per BW, collisions will only occur when two or more EDs transmit data on the same channel frequency and SF at the same time. However, P-ALOHA has limited scalability. With a large number of EDs, the number of collisions greatly increases and channel capacity is reduced significantly.

2.3. MAC schemes for LoRaWAN

Many alternative MAC schemes have been proposed to replace P-ALOHA in LoRaWAN networks. The most promising ones are described next.

2.3.1. Slotted ALOHA

A well-known improvement to the P-ALOHA protocol is Slotted ALOHA (S-ALOHA). With this mechanism, the channel time is split into discrete slots of fixed length and EDs are forced to start their transmissions only at the beginning of a slot. This technique significantly reduces the number of collisions, thus achieving an important increment on channel capacity. In order to define the timeslots required by S-ALOHA, EDs need to maintain their clocks synchronized according to a reference clock. Although providing an efficient synchronization of a large number of EDs is not an easy task due to sparse uplink transmissions, limited downlink availability and different data rates, some promising synchronization schemes have been recently proposed [8,18,21].

2.3.2. CSMA

LoRa chipsets provide a channel activity detection (CAD) mode designed to detect LoRa preamble or data symbols on the radio channel [22]. LoRa CAD procedure usually requires just a few symbols to operate. The exact duration of a CAD measurement depends on the spreading factor, but it is just about the duration of two symbols. This CAD mode can be used to implement a CSMA scheme on top of LoRa [9–14]. With CSMA, EDs must sense the channel before sending their frames. Then, if no activity is detected on the selected channel, the frame transmission can be carried out. Contrarily, if the channel is occupied by an ongoing transmission, EDs must back-off for a random period before checking the channel again. Although CSMA schemes are negatively affected by those transmissions unable to be perceived from hidden nodes, they can alleviate collisions and improve channel capacity in most common scenarios. Another interesting factor that should be taken into account is that stringent duty cycle restrictions enforced by the ETSI to operate in the sub-GHz ISM bands can be bypassed by those MAC protocols that, as CSMA, sense the channel before allowing transmission.

2.3.3. Scheduled time-slotted mechanisms

Several scheduled time-slotted MAC mechanisms have been recently proposed for LoRaWAN networks [15–18]. This kind of mechanisms

[1] Although a perfect orthogonality among SFs is commonly assumed, transmissions from EDs using different SFs may also collide, thus diminishing LoRa performance [20].

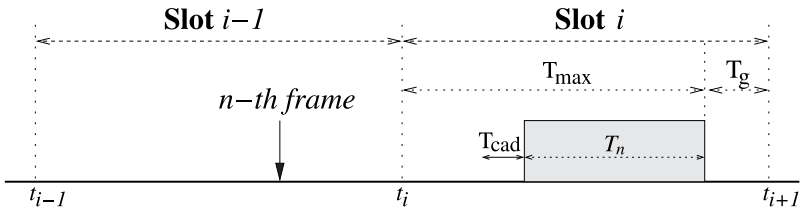

Fig. 1. LFS-CSMA scheduling.

Table 1
MAC schemes for LoRaWAN.

Scheme	Access	Synchronized	CAD
P-ALOHA	Random	No	No
S-ALOHA	Random	Yes	No
CSMA	Random	No	Yes
Scheduled MAC	Reserved	Yes	No
LFS-CSMA	Random	Yes	Yes

splits the channel time in repeated cycles, each one comprising a number of fixed timeslots. Then, each timeslot is allocated to a unique transmitting ED, thus avoiding collisions. As S-ALOHA, these mechanisms require accurate and efficient time synchronization of EDs but, in addition, they also need to implement a resource allocation mechanism, either centralized or distributed. Unfortunately, the scheduling of transmissions is a really challenging task in LoRaWAN networks since they are commonly composed of a dynamic set of heterogeneous EDs, joining and leaving the network at random times, with different (and usually unknown) resource requirements. Moreover, the dissemination of scheduling information to EDs is complicated due to the constrained downlink availability and low data rates. Therefore, although scheduled time-slotted mechanisms have awakened great expectations, they must still address several important issues before being a viable alternative for LoRaWAN networks [19]. For this reason, we have disregarded this kind of mechanisms in the following sections of our study.

Table 1 summarizes the main features of the MAC schemes described in this section. For comparison, it also includes the characteristics of our proposed scheme. As we will show in the next section, LFS-CSMA is able to improve the performance of S-ALOHA by introducing the possibility of performing CAD measurements to reduce the number of collisions.

3. Longest First Slotted CSMA (LFS-CSMA)

This section presents LFS-CSMA, a new MAC protocol for LoRaWAN networks that carefully combines both S-ALOHA and CSMA schemes. First, note that, in time-slotted schemes, the timeslot length should be set to the time required to transmit a frame of maximum size (T_{max}) to avoid frame fragmentation and reassembly operations at the transmitters and receivers, respectively. Additionally, in a real deployment, timeslots must also include a guard interval of length T_g to tolerate slight time de-synchronizations and avoid inter-timeslots collisions. Therefore, we assume that the channel time is split into timeslots of length $T_{slot} = T_{max} + T_g$.

Differently to the classic S-ALOHA scheme, our proposal will not force EDs to start their transmissions at the beginning of a timeslot. Instead, we propose to align frame transmissions at the end of the timeslot, that is, the transmission of each frame will be delayed so that the end of the transmission coincides with the end of the timeslot (without considering the guard time). Thus, since the frames to be sent in a given timeslot presumably have different durations, the longest of them will be transmitted earlier, while EDs with pending frames of shorter sizes will have some time to sense the channel before initiating their own transmissions.

Consider an ED with a frame of length T_n pending to be transmitted at timeslot i, and let t_i be the time at which the timeslot i begins. As shown in Fig. 1, with our scheme, the ED will schedule a CAD measurement of duration T_{cad} at instant $t_i + T_{max} - T_n - T_{cad}$ and, if no channel activity is detected, it will then start the frame transmission at instant $t_i + T_{max} - T_n$. Note that, if the frame duration is so long that $T_{max} - T_{cad} < T_n \leq T_{max}$, then there is not enough time to perform a CAD measurement and the ED must start the transmission of the frame without sensing the channel.

A simple example of S-ALOHA and LFS-CSMA operations with three EDs is shown in Fig. 2. With S-ALOHA, and regardless of frame durations, a successful transmission will occur when only a single ED attempts to transmit in a timeslot, as shown in Fig. 2(a). However, LFS-CSMA takes advantage of the different frame durations to increase the number of successful transmissions. As shown in Fig. 2(b), at the beginning of the first timeslot, ED #1 starts the transmission of a frame of maximum length without carrying out a CAD measurement. Note that this frame is successfully transmitted since EDs #2 and #3 can detect the channel activity before beginning their transmissions and, therefore, can reschedule them to the next timeslot. Then, in the second timeslot, ED #2 successfully transmits its frame after sensing the channel since ED #3 is able to detect the channel activity and cancel its own transmission promptly. However, in the third timeslot, a new frame from ED #1 and the pending one from ED #3 will collide since their sizes (and, therefore, their corresponding transmission instants) are so similar that the CAD procedure of ED #3 is unable to detect the channel activity before initiating transmission.

As can be seen from this example, aligning frame transmissions at the end of the timeslots (instead of aligning them at the beginning, as in S-ALOHA) gives an opportunity to some EDs to detect ongoing transmissions and reschedule their own ones, thus reducing the number of collisions and improving scalability.

4. Performance analysis

In this section we present a new analytical model to evaluate the performance of P-ALOHA, S-ALOHA, CSMA and LFS-CSMA in LoRaWAN networks. Even though it is based on the classic model commonly used to analyze MAC schemes, it has been conveniently adapted to capture the main LoRa features thus providing a realistic model for these networks. A notation summary is provided in Table 2.

Our model will just consider uplink traffic from some unrelated EDs to the GW. We assume perfect orthogonality among SFs and that the number of contending EDs attempting to transmit on the same channel/SF follows a Poisson distribution. Since LoRa frames are allowed to transport payloads of different sizes,[2] we assume that the frame transmission times T_n, for $n = 1, 2, \ldots$, are a set of i.i.d. general random variables with mean $\overline{T}_n = \overline{T}$. We define the normalized load G as the average number of transmission attempts per $\overline{T}$. As the performance measure, we will use the normalized throughput S, defined as the average number of error-free received frames per $\overline{T}$. The normalized throughput can be calculated as the normalized load multiplied by the probability of success of a transmission attempt, that

[2] The PHY header contains a field announcing the payload length.

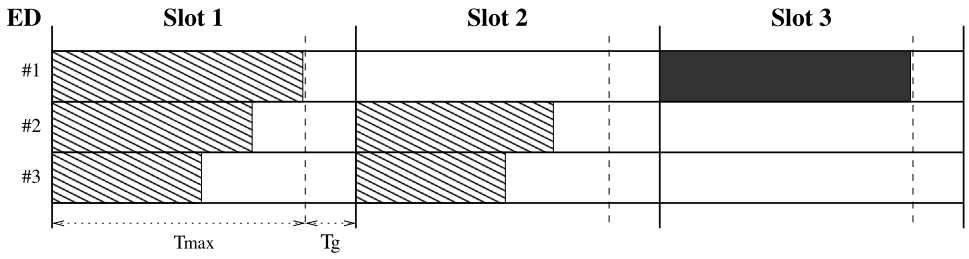

(a) S-ALOHA.

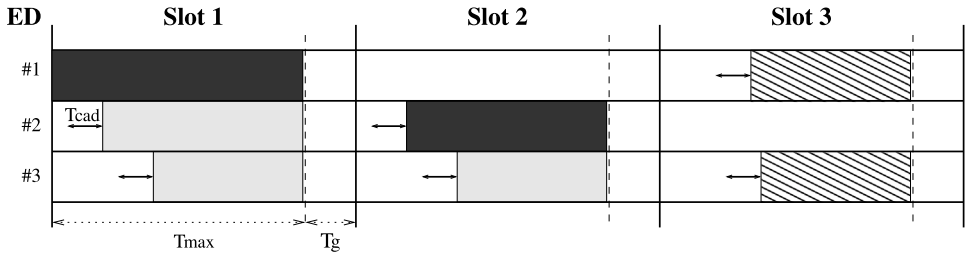

(b) LFS-CSMA.

Fig. 2. S-ALOHA and LFS-CSMA examples. Successfully sent, rescheduled and collided frames are represented with black, gray and dash-filled boxes, respectively.

is, the probability that there are no more transmission attempts during the vulnerability time corresponding to the given MAC protocol. Let V be the vulnerability time, that is, the period during which no further transmissions should be attempted to avoid any collision. Since the number of transmission attempts during a period of length v follows a Poisson distribution of mean $vG/\overline{T}$, then we have that the probability of success of a transmission attempt is

$$p_{\text{success}} = \int_{\mathcal{V}} \mathrm{e}^{-vG/\overline{T}} f_V(v)\,\mathrm{d}v, \tag{1}$$

where $f_V(v)$ is the probability density function of the vulnerability time, and, therefore, the normalized throughput is[3]

$$S = G \cdot p_{\text{success}} = G \int_{\mathcal{V}} \mathrm{e}^{-vG/\overline{T}} f_V(v)\,\mathrm{d}v. \tag{2}$$

Another metric usually employed to evaluate the performance of MAC schemes is the Frame Loss Rate (FLR). This measure is defined as the ratio of unsuccessful transmission attempts, so it can be computed as the complementary probability of a successful transmission attempt:

$$\text{FLR} = 1 - p_{\text{success}} = 1 - \frac{S}{G} = 1 - \int_{\mathcal{V}} \mathrm{e}^{-vG/\overline{T}} f_V(v)\,\mathrm{d}v. \tag{3}$$

Table 2
Notation summary.

Notation	Parameter
G	Normalized load
S	Normalized throughput
V	Vulnerability time
T_n	Transmission time of frame n
$\overline{T}$	Mean frame transmission time
$\mathrm{T_{max}}$	Maximum frame transmission time
$\mathrm{T_{min}}$	Minimum frame transmission time
T_{long}	Transmission time of the longest frame in a timeslot
$\mathrm{T_{sym}}$	Time required to transmit a LoRa symbol
$\mathrm{N_{preamble}}$	Number of symbols comprising the LoRa preamble
$\mathrm{T_{preamble}}$	Time required to transmit the LoRa preamble
$\mathrm{N_{phy}}$	Number of symbols comprising the physical message
$\mathrm{T_{phy}}$	Time required to transmit the physical message
$\mathrm{T_{olap}}$	Time allowing overlapped LoRa preamble transmissions
G_{olap}	Mean number of transmission attempts in a $\mathrm{T_{olap}}$ period
$\mathrm{T_g}$	Guard time (in slotted schemes)
$\mathrm{T_{slot}}$	Timeslot length (in slotted schemes)
G_{slot}	Mean number of transmission attempts in a timeslot
$\mathrm{T_{cad}}$	Time required for a CAD measurement
G_{cad}	Mean number of transmission attempts in a $\mathrm{T_{cad}}$ period
ρ_{h}	Ratio of hidden EDs
R	LoRa data rate

4.1. P-ALOHA

It is well known that, in a pure Aloha system, a frame will be successfully transmitted:

1. if the number of uncompleted preceding transmissions at the beginning of the reference transmission is zero,
2. and if no node starts a new transmission during the reference transmission time.

However, several studies have shown the ability of LoRa to receive partially overlapped transmissions [23]. In fact, LoRa receivers are able to correctly decode a frame even if the first preamble symbols collide with other transmissions granted that at least six symbols are not overlapped. Then, the first condition happens with probability

$$p_1 = \mathrm{e}^{-(\overline{T}-\mathrm{T_{olap}})G/\overline{T}} = \mathrm{e}^{-(G-G_{\text{olap}})}, \tag{4}$$

where $G_{\text{olap}} = G\mathrm{T_{olap}}/\overline{T}$ is the mean number of transmission attempts in a $\mathrm{T_{olap}}$ period, $\mathrm{T_{olap}} = \mathrm{T_{preamble}} - 6\mathrm{T_{sym}}$ is the time LoRa allows overlapped preamble transmissions, $\mathrm{T_{preamble}}$ is the time required to transmit the LoRa preamble symbols and $\mathrm{T_{sym}}$ is the duration of a symbol.[4] On the other hand, assuming i.i.d. transmission times with probability density function $f_T(t)$, the second condition is met with

[3] We will disregard the effect of the variable success probability for different frame sizes on the mean carried traffic and focus on throughput instead.

[4] Appendix A shows how to compute these values for a particular LoRa configuration.

probability

$$p_2 = \int_{\mathcal{T}} \mathrm{e}^{-tG/\overline{T}} f_T(t)\,\mathrm{d}t. \tag{5}$$

Therefore, the probability of success of a transmission attempt is $p_{\text{success}} = p_1 p_2$ and the normalized throughput is given by

$$S_{\text{P-ALOHA}} = G\mathrm{e}^{-(G-G_{\text{olap}})} \int_{\mathcal{T}} \mathrm{e}^{-tG/\overline{T}} f_T(t)\,\mathrm{d}t. \tag{6}$$

4.2. S-ALOHA

Thanks to the introduction of discrete timeslots, S-ALOHA reduces the vulnerability time to just one timeslot duration. Recall that the timeslot length should be enough to transmit a frame of maximum size plus a guard interval ($\mathrm{T}_{\text{slot}} = \mathrm{T}_{\text{max}} + \mathrm{T}_{\text{g}}$). Therefore, assuming that the guard interval is large enough so that the probability of collision in adjacent timeslots is negligible, the vulnerability time with S-ALOHA is then $V_{\text{S-ALOHA}} = \mathrm{T}_{\text{slot}} = \mathrm{T}_{\text{max}} + \mathrm{T}_{\text{g}}$ and the normalized throughput is given by

$$S_{\text{S-ALOHA}} = G\mathrm{e}^{-G_{\text{slot}}}, \tag{7}$$

where $G_{\text{slot}} = G\mathrm{T}_{\text{slot}}/\overline{T}$ is the mean number of transmission attempts in a timeslot. Note that the throughput obtained with this scheme is independent of the distribution of the transmission times. Finally, it should also be noticed that S-ALOHA is not able to take advantage of the ability of LoRa to receive partially overlapped transmissions since all of them are initiated at the beginning of the timeslot.

4.3. CSMA

CSMA-based schemes can be implemented using the CAD mode embedded in LoRa chipsets. Unfortunately, it has been reported that, under some radio conditions, the CAD procedure fails to detect channel activity in real-world deployment scenarios [13], so it is recommended to take several consecutive CAD measurements to improve activity detection accuracy [24]. In any case, it must be taken into account that CAD unreliability and the existence of hidden terminals hinder the efficiency of CSMA approaches.

Certainly, the CAD mode will be able to detect an ongoing LoRa transmission just as soon as the radio signal from that transmission reaches the listening ED. However, note that propagation delays in LoRaWAN networks are much shorter than the duration of a symbol transmission (and, therefore, than the duration of the CAD procedure, T_{cad}), so they are usually neglected when analyzing this kind of networks. We thus assume that two transmission attempts will not collide if the elapsed time between them is longer than T_{cad} and the sending EDs can hear each other. Taking this into account, a LoRa frame will be successfully transmitted with a non-persistent CSMA scheme when the four following independent conditions are simultaneously met:

1. There are no more transmission attempts during the initial T_{cad} period following the beginning of the reference transmission. This happens with probability $p_1 = \mathrm{e}^{-G_{\text{cad}}}$, where $G_{\text{cad}} = G\mathrm{T}_{\text{cad}}/\overline{T}$ is the mean number of transmission attempts during a CAD measurement.
2. There are no more transmissions attempts from hidden EDs during the transmission time remaining after the initial T_{cad} period following the beginning of the reference transmission. Let ρ_{h} be the ratio of hidden EDs from the sending ED. We assume for simplicity that all EDs observe the same constant ρ_{h} ratio. Then, this condition is met with probability
$$p_2 = \int_{\mathcal{T}} \mathrm{e}^{-(t-\mathrm{T}_{\text{cad}})\rho_{\text{h}}G/\overline{T}} f_T(t)\,\mathrm{d}t = \mathrm{e}^{\rho_{\text{h}}G_{\text{cad}}} \int_{\mathcal{T}} \mathrm{e}^{-t\rho_{\text{h}}G/\overline{T}} f_T(t)\,\mathrm{d}t. \tag{8}$$
3. The number of uncompleted preceding transmissions from hidden EDs at the beginning of the reference transmission is zero. Recall that LoRa allows overlapped preamble transmissions for a T_{olap} period, so this condition is met with probability
$$p_3 \approx \mathrm{e}^{-(\overline{T}-\mathrm{T}_{\text{olap}})\rho_{\text{h}}G/\overline{T}} = \mathrm{e}^{-\rho_{\text{h}}(G-G_{\text{olap}})}. \tag{9}$$
4. The CAD procedure of the sending ED has not detected any activity on the selected channel since, otherwise, it would not have sent the frame. Let p_{free} be the probability that an ED finds the channel free after a CAD measurement. We will compute this probability as $p_{\text{free}} = 1 - p_{\text{busy}}$, where p_{busy} is the probability that an ongoing transmission is detected, that is, the probability that a frame is being transmitted from a no hidden ED. This probability can be approximated as $p_{\text{busy}} \approx n_{\text{tx}} p_{\text{tx}}$, with p_{tx} being the probability that at least one transmission will be carried out after a CAD measurement and n_{tx} the mean number of independent periods of length T_{cad} that comprises a frame transmission, if we assume that once a frame is transmitted in one of these T_{cad} periods, any other transmission attempt in the following ones will be canceled. Note that a transmission will be carried out after a T_{cad} period if the channel is sensed free (again with probability p_{free}) and if there is at least one transmission attempt from a no hidden ED in this period, so $p_{\text{tx}} = p_{\text{free}}(1-\mathrm{e}^{-(1-\rho_{\text{h}})G_{\text{cad}}})$. Since n_{tx} can be obtained as $\overline{T}/\mathrm{T}_{\text{cad}}$, then we have that
$$p_{\text{free}} = 1 - \frac{\overline{T}}{\mathrm{T}_{\text{cad}}} p_{\text{free}}(1-\mathrm{e}^{-(1-\rho_{\text{h}})G_{\text{cad}}}), \tag{10}$$
and solving for p_{free}, we get that
$$p_{\text{free}} = \frac{\mathrm{T}_{\text{cad}}}{\mathrm{T}_{\text{cad}} + \overline{T}\left(1-\mathrm{e}^{-(1-\rho_{\text{h}})G_{\text{cad}}}\right)}. \tag{11}$$

The success probability of a transmission attempt is, therefore, $p_{\text{success}} = p_1 p_2 p_3 p_{\text{free}}$, and we have that

$$S_{\text{CSMA}} = \frac{G_{\text{cad}}\,\mathrm{e}^{-\rho_{\text{h}}(G-G_{\text{olap}})-(1-\rho_{\text{h}})G_{\text{cad}}}}{1+G_{\text{cad}}/G-\mathrm{e}^{-(1-\rho_{\text{h}})G_{\text{cad}}}} \int_{\mathcal{T}} \mathrm{e}^{-t\rho_{\text{h}}G/\overline{T}} f_T(t)\,\mathrm{d}t. \tag{12}$$

4.4. LFS-CSMA

Clearly, the vulnerability time with our proposal is again equal to one timeslot duration. However, note that, now, not every transmission attempt will be eventually carried out, since those EDs detecting channel activity through the CAD procedure will postpone their scheduled transmissions. Certainly, within a given timeslot, the ED with the longest frame to be sent will be the one that schedules the earliest frame transmission. Consequently, it will not sense any activity on the channel and will eventually start the transmission of the frame at the corresponding instant. This transmission, of duration T_{long}, will be successful if the rest of EDs with pending frames in the timeslot are able to detect it and defer their transmission attempts, that is, if all the rest of pending frames in the timeslot correspond to no hidden EDs and have a duration smaller than $T_{\text{long}} - \mathrm{T}_{\text{cad}}$.

Assume that there are $1 + k$ frames waiting to be sent in a given timeslot, all of them with i.i.d. lengths (the longest frame and the remaining k ones). Clearly, if $k = 0$, the unique frame in the timeslot will always be successfully transmitted. Otherwise, the probability that a different ED (of the remaining k EDs with a frame to be sent) can detect the ongoing transmission can be computed as

$$p_{\text{cad}} = (1-\rho_{\text{h}})F_{T'}(T_{\text{long}} - \mathrm{T}_{\text{cad}}), \tag{13}$$

where $F_{T'}(t)$ is the cumulative distribution function of the random variable T' that represents the transmission time of those frames shorter than the longest one in the timeslot ($T' = T \mid T < T_{\text{long}}$). On the other hand, as shown in Appendix B, the cumulative distribution function of the length of the longest frame in the timeslot is $F_{T_{\text{long}}}(t) = \left(F_T(t)\right)^{1+k}$, and hence, differencing it, we get that its probability density function

Table 3
Configuration parameters.

Parameter	Dense scenario	Sparse scenario
SF	7	10
BW	125 kHz	125 kHz
CR	4/5	4/5
T_{sym}	1.024 ms	8.192 ms
$N_{preamble}$	8 symbols	8 symbols
$T_{preamble}$	12.544 ms	100.352 ms
$N_{payload}$	85–115 bytes	25–51 bytes
N_{phy}	133–178 symbols	38–63 symbols
T_{min}	148.736 ms	411.648 ms
T_{max}	194.816 ms	616.448 ms
$\overline{T}$	171.776 ms	514.048 ms
T_g	9.741 ms	30.823 ms
T_{slot}	204.557 ms	647.271 ms
T_{cad}	4.096 ms	32.768 ms
R	5.469 kb/s	0.977 kb/s
ρ_h	0.05	0.1

is $f_{T_{long}}(t) = (1+k)\left(F_T(t)\right)^k f_T(t)$. Then, the probability that all the k remaining EDs in the timeslot detect the transmission of the longest frame and avoid the collision is

$$p_{cad}(k) = \int_{\mathcal{T}} \left((1-\rho_h)F_{T'}(t-T_{cad})\right)^k f_{T_{long}}(t)\,dt$$
$$= (1+k)(1-\rho_h)^k \int_{\mathcal{T}} \left(F_{T'}(t-T_{cad})\right)^k \left(F_T(t)\right)^k f_T(t)\,dt, \quad (14)$$

and, therefore, the probability of success is given by

$$p_{success} = e^{-G_{slot}} + \sum_{k=1}^{\infty} \frac{(G_{slot})^k e^{-G_{slot}}}{k!} \cdot \frac{p_{cad}(k)}{1+k} \quad (15)$$

since $1/(1+k)$ is the probability that the frame is the longest one in the timeslot. Finally, recall that the success probability must be multiplied by the normalized load to get the normalized throughput as usual.

5. Numerical results

For the performance evaluation of the MAC schemes analyzed in the previous section, we have considered two different scenarios. In the first one, a dense LoRaWAN network with EDs close to the GW was assumed, so it was configured with the lowest spreading factor (SF = 7) to reduce energy consumption and achieve high data rates. In the second scenario, we considered a sparse LoRaWAN network where EDs are farther from the GW, so it was configured with a higher spreading factor (SF = 10) to provide a longer range connectivity. Table 3 shows the main LoRa configuration parameters for both scenarios. We selected the default values intended for EU868 band and assumed uniformly distributed payload sizes up to the maximum possible values for each configuration scenario according to LoRa restrictions for the given SFs. For the slotted schemes, we considered a guard time equal to 5% of T_{max} while, for the CSMA-based techniques, we fixed T_{cad} to the duration of 4 symbols. Finally, note that the ratio of hidden EDs configured for the sparse scenario doubles that configured for the dense one.

We have particularized in Appendix C the model developed in Section 4 assuming uniform frame transmission times. The graphs in the following subsections show the numerical results obtained when applying the formulas derived in Appendix C to both the considered scenarios.

5.1. Dense scenario

Fig. 3(a) shows the normalized throughput achieved in the dense scenario for the different MAC schemes with normalized loads up to 1. Firstly, note that, as expected, S-ALOHA improves the throughput achieved with P-ALOHA thanks to the introduction of timeslots. However, when the traffic load increases, the ability to detect the channel activity before transmitting frames permits reducing the amount of collisions significantly and both CSMA-based schemes obtain higher normalized throughputs than the Aloha-based ones at both medium and high loads, although LFS-CSMA is the scheme that provides the best performance.

FLRs obtained for the different schemes are compared in Fig. 3(b). Note that, even for a modest target FLR of just 0.1, P-ALOHA could only perform at very low loads ($G \approx 0.054$), while S-ALOHA and CSMA would be able to support a traffic load up to $G \approx 0.088$ and 0.103, respectively. Our proposal clearly outperforms all these schemes since, for the selected target FLR, it is able to support a load close to $G \approx 0.148$.

5.2. Sparse scenario

Fig. 4 depicts the results obtained for the sparse scenario. As expected, these are very similar to those obtained for the dense one with just some nuances. Again, CSMA-based schemes achieve more throughput than Aloha-based ones. Also, note that the throughput that can be obtained with both CSMA-based schemes has been reduced since the ratio of hidden EDs is much higher in this scenario. In any case, our scheme is again the one that gets the highest throughput.

Regarding the FLRs, these are also very similar to those obtained in the dense scenario. Now, the traffic loads that the schemes can support to maintain a target FLR of 10^{-1} are, approximately, 0.055, 0.084, 0.095 and 0.123 for P-ALOHA, S-ALOHA, CSMA and LFS-CSMA, respectively. In view of these results, we can affirm that the proposed LFS-CSMA scheme can significantly improve the scalability of LoRaWAN networks just introducing limited complexity.

5.3. Fairness

Not surprisingly, LFS-CSMA introduces a fairness bias in favor of long frames. Recall that our scheme inherently selects for transmission the longest frame in each timeslot. As shown in (13), the longer the longest frame in the timeslot is, the higher the probability of transmission detection and, therefore, the higher the probability of transmission success.

However, this bias is not a great concern in practical scenarios. To show this, we have derived the probability of success in the transmission of a frame as a function of its duration (see Appendix C.3.1) and computed this probability for the minimum, average and maximum frame durations considered in both the dense and sparse scenarios (see Table 3). Maximum payload sizes have been selected according to LoRa restrictions for the given SFs in the EU868 band, while the corresponding frame durations for each payload size have been calculated using the formulas shown in Appendix A, as established in LoRa specification. Fig. 5 shows the normalized success probabilities for the minimum and the average frame durations in each scenario (that is, their success probabilities divided by the success probability of the longest frames). Certainly, shorter frames experience smaller success probabilities. However, note that the impact of frame duration on the success probability increases with network load. In fact, the reduction in the success probability obtained for moderate (and most common) loads is relatively low and, therefore, the effects of this bias are limited in practice. On the other hand, it is expected that, after a backoff period, the amount of pending data in the ED will increase, thus enlarging the size of the pending frame and, therefore, its transmission priority.

Finally, it can also be argued that, as in practice this bias only has a negative impact on the delay experienced by short frames, it would be almost irrelevant in scenarios with flexible delay requirements. Moreover, prioritizing long frames may be the appropriate behavior for this kind of mechanisms since, as they transport more data, this has a beneficial effect on the amount of carried traffic and, therefore, on the whole network efficiency.

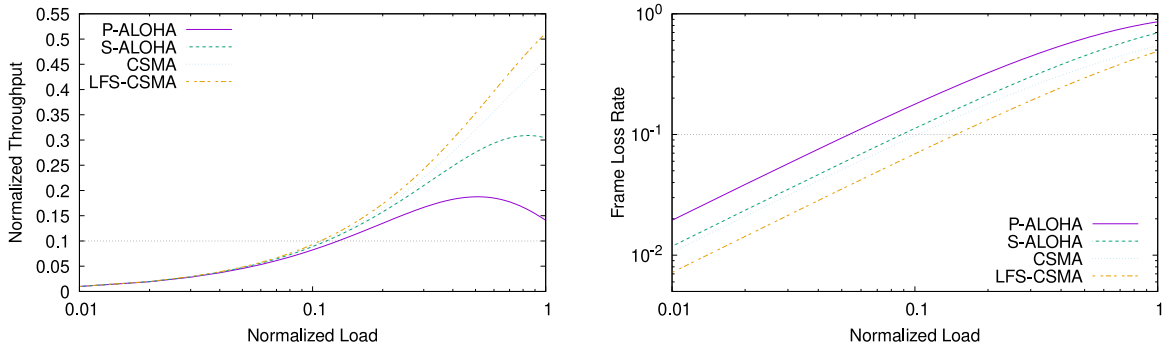

(a) Normalized throughput. (b) Frame loss rate.

Fig. 3. Dense scenario results.

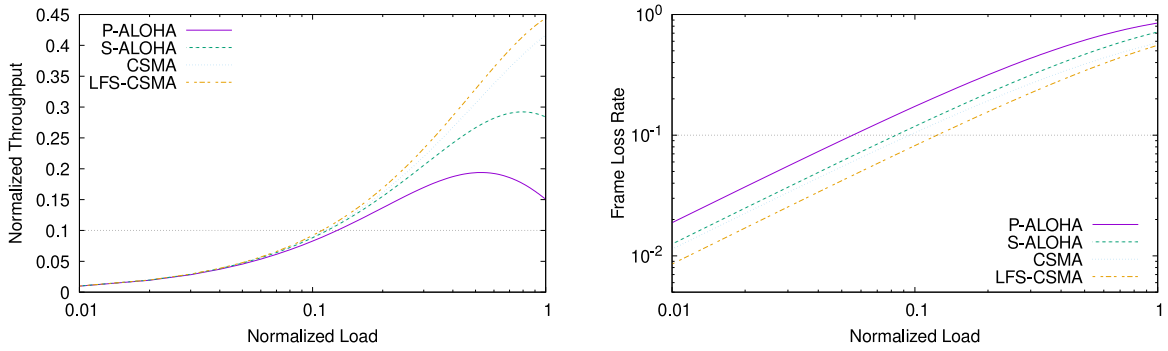

(a) Normalized throughput. (b) Frame loss rate.

Fig. 4. Sparse scenario results.

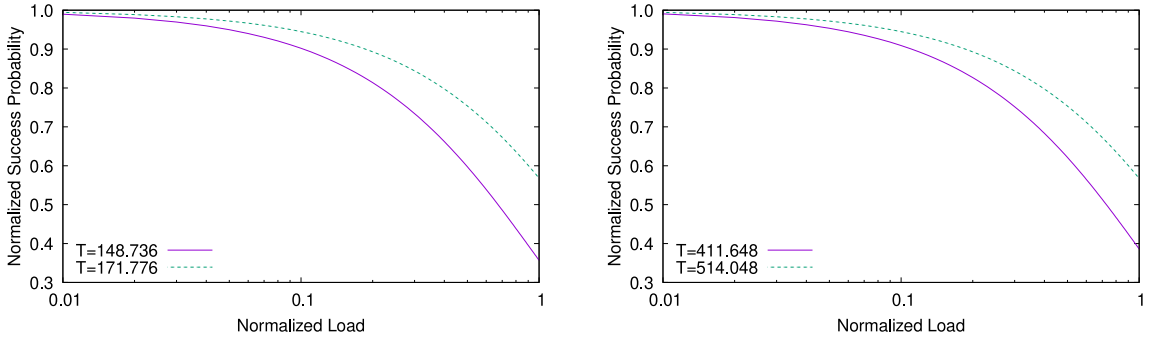

(a) Dense scenario ($T_{max} = 194.816$ ms). (b) Sparse scenario ($T_{max} = 616.448$ ms).

Fig. 5. Normalized transmission success probability.

5.4. Energy efficiency

Finally, we also evaluated the energy efficiency of the MAC schemes. We define the energy efficiency η as the average number of bits that EDs can successfully transmit through the channel per joule:

$$\eta = \frac{S\,\overline{N}_{\text{success}}}{G\,\overline{\text{E}} + \text{P}_{\text{sync}}}, \tag{16}$$

where $\overline{N}_{\text{success}}$ is the average number of bits in the payload of the frames that are successfully transmitted, $\overline{\text{E}}$ is the average energy required to deliver a frame to the GW and P_{sync} is the power consumed by the synchronization procedure in the slotted schemes.

The $\overline{N}_{\text{success}}$ for each MAC scheme has been computed in Appendix D. Regarding the energy required to send a frame, note that, with ALOHA-based schemes, EDs just consume energy when transmitting frames. Then, if P_{tx} is the power consumption of an ED while transmitting, the average energy required for each transmission attempt is $\overline{\text{E}}_{\text{P-ALOHA}} = \overline{\text{E}}_{\text{S-ALOHA}} = \text{P}_{\text{tx}}\overline{T}$. However, with CSMA and LFS-CSMA, frames are only transmitted when the channel is sensed free (with some probability p_{free}), although EDs must consume some additional energy when performing CAD measurements, so $\overline{\text{E}}_{\text{CSMA}} = \overline{\text{E}}_{\text{LFS-CSMA}} =$

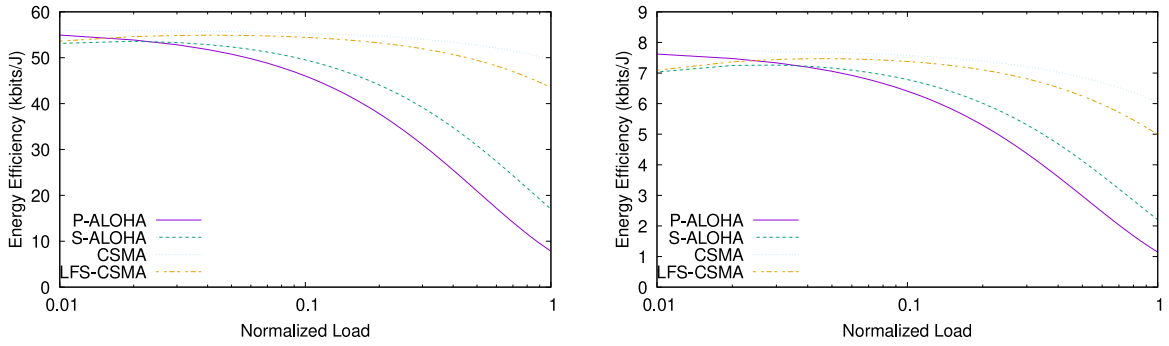

(a) Dense scenario. (b) Sparse scenario.

Fig. 6. Energy efficiency.

$p_{\text{free}} P_{\text{tx}} \overline{T}_{\text{tx}} + P_{\text{rx}} T_{\text{cad}}$, where $\overline{T}_{\text{tx}}$ is the average duration of the transmitted frames and P_{rx} is the power consumption of an ED while sensing the channel. The p_{free} probability with CSMA has already been computed in (11), while, for the LFS-CSMA scheme, we have obtained it in Appendix C.3.2. Regarding the duration of the frames sent, note that, for low ratios of hidden EDs, we have that $\overline{T}_{\text{tx}} \approx \overline{T}$ with CSMA and $\overline{T}_{\text{tx}} \approx \overline{T}_{\text{long}}$ with LFS-CSMA. The average duration of the longest frame in a timeslot has been computed in Appendix D.3.

Additionally, both S-ALOHA and LFS-CSMA schemes require some extra energy to keep EDs synchronized. Assuming that synchronization is performed by the reception of periodic beacons with payload size N_{beacon} (and corresponding duration T_{beacon}) sent by the GW at intervals of length T_{sync}, we have that $P_{\text{sync}} = P_{\text{rx}} T_{\text{beacon}} / T_{\text{sync}}$.

Fig. 6 shows the energy efficiency obtained in both dense and sparse scenarios using the same energy parameters as in [25]: $P_{\text{tx}} = 84.15\,\text{mW}$, $P_{\text{rx}} = 15.18\,\text{mW}$, $N_{\text{beacon}} = 16\,\text{B}$ and $T_{\text{sync}} = 128\,\text{s}$. Clearly, CSMA and LFS-CSMA are the most energy efficient MAC schemes. Channel activity detection improves energy efficiency since frames are only transmitted when the channel is sensed free, thus reducing the number of useless transmissions significantly. These graphs also show that our scheme improves the throughput of LoRa networks at the cost of slightly increasing energy consumption with respect to CSMA. In any case, the loss of energy efficiency is minor and is clearly compensated by the higher throughput. Finally, note that the sparse scenario is more energy demanding than the dense one. This is mainly due to the fact that the frames in the sparse scenario must transport shorter payloads to reach longer distances.

6. Discussion

In this section we discuss some relevant issues for deploying LFS-CSMA. First, recall that, as every slotted time-based scheme, LFS-CSMA must rely on an efficient and accurate synchronization system to define the timeslots. In particular, for our scheme it suffices with a lightweight synchronization mechanism that guarantees time differences below a few milliseconds. Several synchronization mechanisms such as those proposed in [8,18,21] fulfill these requirements, so any of them could be satisfactorily employed with our scheme.

Another important aspect to be considered is the duration of the timeslots. We claim in Section 3 that the timeslot length must be set to the time required to transmit a frame of maximum size plus a guard time to tolerate slight de-synchronizations. The maximum frame duration can be easily pre-computed considering the maximum payload size according to LoRa restrictions for the employed SFs and frequency bands, or the maximum application payload size, if known. Regarding the guard time, its actual value depends on both the accuracy of the synchronization mechanism and the maximum propagation delay but, for all the considered mechanisms and scenarios, it would be equivalent to a very small portion of the whole timeslot duration. Therefore, EDs could be preconfigured with a suitable fixed timeslot duration without the need to exchange any overhead traffic to disseminate this information among them.

Also note that our proposal benefits from the fact that EDs send frames of different durations to perform CAD measurements before frame transmissions and thus avoid collisions. However, if all frames have the same duration, all EDs will start their transmissions at the same instant and LFS-CSMA degenerates into a classical S-ALOHA scheme. In any case, this is a very improbable scenario. It can be proved from (A.2) that a small difference in the payload sizes of LoRa frames results in a sufficiently large difference in the number of LoRa symbols so as to permit that the EDs sending slightly shorter frames can perform a CAD measurement. For example, a difference of just two bytes in the payload sizes leads to a significant difference of five symbols in the respective LoRa frames, thus leaving enough time to carry out a complete CAD measurement, as explained in Section 2.3.2.

Finally, we would like to point out that the existence of multiple gateways in the LoRa network is irrelevant from the point of view of our scheme. Frequently, several gateways must be deployed in large-scale LoRa networks to provide connectivity to the EDs. However, in these scenarios, the EDs are not associated to a particular GW, but broadcast their frames to all the GWs in their transmission range. The GWs then act as relays just forwarding the data to a network server that filters out the duplicate messages and selects the GW to be used for downlink transmission. Therefore, our scheme is not affected by the presence of several GWs since its goal is just to increase the throughput to a given GW on a specific channel/SF.

7. Conclusions

We have presented in this paper LFS-CSMA, a new MAC scheme that improves the scalability of LoRaWAN networks by just combining the well-known slotted Aloha and CSMA mechanisms in a novel manner. To reduce the amount of collisions when the network load increases, our proposal transmits frames within a given timeslot at different instants according to their lengths. In particular, LFS-CSMA transmits longer frames earlier, thus leaving to those EDs with frames of shorter sizes some time to perform a CAD measurement before initiating their transmissions, so that they can reschedule them if the channel is busy.

To evaluate the performance of our proposal and compare it with other random access MAC mechanisms, we have also developed an analytical model that captures main LoRa features. Performance results show that LFS-CSMA outperforms all the considered MAC mechanisms improving the scalability of LoRa transmissions significantly.

CRediT authorship contribution statement

Sergio Herrería-Alonso: Conceptualization, Methodology, Writing – original draft. **Andrés Suárez-González:** Validation, Formal analysis. **Miguel Rodríguez-Pérez:** Writing – review & editing, Project administration. **Cándido López-García:** Supervision.

Declaration of competing interest

The authors declare that they have no known competing financial interests or personal relationships that could have appeared to influence the work reported in this paper.

Data availability

No data was used for the research described in the article.

Acknowledgments

This work has received financial support from grant PID2020-113240RB-I00, financed by MCIN/AEI/10.13039/501100011033, and by the Xunta de Galicia (Centro singular de investigación de Galicia accreditation 2019–2022) and the European Union (European Regional Development Fund—ERDF). Funding for open access charge: Universidade de Vigo/CISUG.

Appendix A. LoRa frame duration and data rate

The duration of a LoRa frame transmission (also referred as *time on air*, ToA) depends on several configurable radio parameters: the spreading factor (SF $\in \{7,8,\dots,12\}$), the bandwidth (BW) and the coding rate (CR $\in \{4/5, 4/6, 4/7, 4/8\}$). It can be obtained as the sum of the times required to transmit the preamble ($T_{preamble}$) and the physical message (T_{phy}):

$$\text{ToA} = T_{preamble} + T_{phy} = T_{sym} \cdot (N_{preamble} + 4.25 + N_{phy}), \tag{A.1}$$

where $T_{sym} = 2^{SF}/BW$ is the duration of a symbol, $N_{preamble}$ is the number of symbols of the configurable part of the preamble and

$$N_{phy} = 8 + \left\lceil \frac{44 + 8 \cdot N_{payload} - 4 \cdot SF}{4(SF - 2 \cdot DE)} \right\rceil \cdot \frac{4}{CR} \tag{A.2}$$

is the number of symbols comprising the physical message when it includes the CRC field. In this expression, $N_{payload}$ denotes the payload size (in bytes) and DE represents if the low data rate optimization is enabled (DE = 1 if SF $\in \{11, 12\}$, DE = 0 otherwise).

LoRa data rate R also depends on the SF, BW and CR parameters. It can be calculated as follows:

$$R = CR \cdot \frac{SF}{T_{sym}}. \tag{A.3}$$

Appendix B. Probability distribution of the maximum value of a number of uniform random variables

Consider a sequence $\{X_1, X_2, \dots, X_n\}$ of independent random variables with common cumulative distribution function (CDF) $F_{X_i}(x) = F_X(x)$ and let $Y = \max\{X_1, X_2, \dots, X_n\}$. Then, for any fixed n, the CDF of Y is given by

$$F_Y(y) = P[Y \le y] = P[X_1 \le y, X_2 \le y, \dots, X_n \le y] = \big(F_X(y)\big)^n, \tag{B.1}$$

since all X_i's are independent. Particularizing for the case when all X_i's are Uniform(a, b), we have that

$$F_Y(y) = \begin{cases} 0 & y \le a, \\ \left(\frac{y-a}{b-a}\right)^n & a < y < b, \\ 1 & y \ge b, \end{cases} \tag{B.2}$$

and hence, differencing it, we get that the probability density function of Y is

$$f_Y(y) = n \frac{(y-a)^{n-1}}{(b-a)^n}, \quad a \le y \le b. \tag{B.3}$$

Appendix C. Normalized throughput with uniform transmission times

In Section 4 we developed an analytical model to evaluate the performance of the MAC schemes assuming that the number of transmission attempts follows a Poisson distribution and that frame transmission times are i.i.d. and follow a general distribution of mean $\overline{T}$. In this appendix we particularize this model assuming uniformly distributed transmission times in the range $[T_{min}, T_{max}]$. For the uniform distribution, we have that $f_T(t) = 1/\Delta_T$ with $\Delta_T = T_{max} - T_{min}$ and $\overline{T} = (T_{min} + T_{max})/2$. Also recall that, as shown in (7), S-ALOHA throughput is independent of the distribution of the transmission times, so we can disregard this scheme here.

C.1. P-ALOHA

Substituting $f_T(t) = 1/\Delta_T$ in (6), we get that

$$\begin{aligned} S_{\text{P-ALOHA}} &= G e^{-(G-G_{olap})} \int_{T_{min}}^{T_{max}} e^{-tG/\overline{T}} \frac{1}{\Delta_T} \, dt \\ &= \frac{G e^{-(G-G_{olap})}}{G_{\Delta T}} \left(e^{-G_{min}} - e^{-G_{max}}\right), \end{aligned} \tag{C.1}$$

where $G_{min} = G T_{min}/\overline{T}$ and $G_{max} = G T_{max}/\overline{T}$ are the mean number of transmission attempts during the transmission of a frame of minimum and maximum length, respectively, and $G_{\Delta T} = G\Delta_T/\overline{T}$ is the mean number of transmission attempts during a Δ_T period.

C.2. CSMA

Substituting $f_T(t) = 1/\Delta_T$ in (12), we get that

$$\begin{aligned} S_{\text{CSMA}} &= \frac{G_{cad}\, e^{-\rho_h(G-G_{olap})-(1-\rho_h)G_{cad}}}{1 + G_{cad}/G - e^{-(1-\rho_h)G_{cad}}} \int_{T_{min}}^{T_{max}} e^{-t\rho_h G/\overline{T}} \frac{1}{\Delta_T} \, dt \\ &= \frac{G_{cad}\, e^{-\rho_h(G-G_{olap})-(1-\rho_h)G_{cad}}}{1 + G_{cad}/G - e^{-(1-\rho_h)G_{cad}}} \cdot \frac{e^{-\rho_h G_{min}} - e^{-\rho_h G_{max}}}{\rho_h G_{\Delta T}}. \end{aligned} \tag{C.2}$$

C.3. LFS-CSMA

Substituting $f_T(t) = 1/\Delta_T$, $F_T(t) = (t - T_{min})/\Delta_T$ and $F_{T'}(t) = (t - T_{min})/(T_{long} - T_{min})$ in (14), we have that

$$\begin{aligned} p_{cad}(k) &= (1+k)(1-\rho_h)^k \int_{T_{min}+T_{cad}}^{T_{max}} \left(\frac{t - T_{cad} - T_{min}}{t - T_{min}} \cdot \frac{t - T_{min}}{\Delta_T}\right)^k \frac{1}{\Delta_T} \, dt \\ &= \frac{(1+k)(1-\rho_h)^k}{\Delta_T^{1+k}} \int_{T_{min}+T_{cad}}^{T_{max}} (t - T_{cad} - T_{min})^k \, dt \\ &= (1-\rho_h)^k (1-c)^{1+k}, \end{aligned} \tag{C.3}$$

with $c = T_{cad}/\Delta_T$. Then, substituting this in (15), we get that

$$\begin{aligned} p_{success} &= e^{-G_{slot}} + \sum_{k=1}^{\infty} \frac{(G_{slot})^k e^{-G_{slot}}}{k!} \cdot \frac{(1-\rho_h)^k (1-c)^{1+k}}{1+k} \\ &= \frac{e^{-G_{slot}}}{(1-\rho_h)G_{slot}} \left(e^{(1-c)(1-\rho_h)G_{slot}} + c(1-\rho_h)G_{slot} - 1\right). \end{aligned} \tag{C.4}$$

C.3.1. Transmission success probability as a function of frame length

To evaluate the fairness bias introduced by our scheme in favor of long frames, we have also computed the probability of success in the transmission of a frame as a function of its length. As shown in Section 4.4, a frame requiring a transmission time T_n will be successfully transmitted if it is the longest one in the timeslot and all the rest of pending frames correspond to no hidden EDs and have a duration shorter than $T_n - T_{cad}$. Thus, assuming that there are $1+k$ frames waiting to be sent in the timeslot, the probability p_{long} that the given frame is the longest one in the timeslot is

$$p_{long}(k, T_n) = \left(\frac{T_n - T_{min}}{T_{max} - T_{min}}\right)^k, \tag{C.5}$$

that is, the probability that the remaining k frames in the timeslot last less than T_n. On the other hand, the probability that the other k EDs with pending frames can detect its transmission is

$$p_{\text{cad}}(k,T_n) = (1-\rho_{\text{h}})^k \left(F_{T'}(T_n - \text{T}_{\text{cad}})\right)^k = (1-\rho_{\text{h}})^k \left(\frac{T_n - \text{T}_{\text{cad}} - \text{T}_{\text{min}}}{T_n - \text{T}_{\text{min}}}\right)^k, \tag{C.6}$$

if $T_n > \text{T}_{\text{min}} + \text{T}_{\text{cad}}$ (or 0, otherwise). Therefore,

$$p_{\text{success}}(T_n) = \text{e}^{-G_{\text{slot}}} + \sum_{k=1}^{\infty} \frac{(G_{\text{slot}})^k \text{e}^{-G_{\text{slot}}}}{k!} \cdot p_{\text{cad}}(k,T_n) \cdot p_{\text{long}}(k,T_n). = \text{e}^{-G_{\text{slot}}(1-(1-\rho_{\text{h}})(T_n-\text{T}_{\text{cad}}-\text{T}_{\text{min}})/(\text{T}_{\text{max}}-\text{T}_{\text{min}}))}, \tag{C.7}$$

if $T_n > \text{T}_{\text{min}} + \text{T}_{\text{cad}}$ (or $\text{e}^{-G_{\text{slot}}}$, otherwise).

C.3.2. Frame transmission probability

With our proposal, an ED will eventually send a frame if it previously finds the channel free after a CAD measurement. This will occur when (*a*) the pending frame is the longest one in the timeslot, or (*b*) the ED is unable to detect the transmission of the longest frame, either because (*b1*) the duration of its pending frame is greater than $T_{\text{long}} - \text{T}_{\text{cad}}$, or because (*b2*) the transmitting node is a hidden ED. Therefore, if there are $1+k$ frames waiting to be sent in a timeslot, then the probability that the channel is sensed free can be computed as

$$\begin{aligned} p_{\text{free}}(k) &= \frac{1}{1+k} + \frac{k}{1+k}\int_{\mathcal{T}} \left(1 - F_{T'}(t-\text{T}_{\text{cad}}) + \rho_{\text{h}} F_{T'}(t-\text{T}_{\text{cad}})\right) f_{T_{\text{long}}}(t)\,\text{d}t \\ &= \frac{1}{1+k} + \frac{k}{1+k}\int_{\mathcal{T}} \left(1-(1-\rho_{\text{h}})F_{T'}(t-\text{T}_{\text{cad}})\right)(1+k)\left(F_T(t)\right)^k f_T(t)\,\text{d}t \\ &= \frac{1}{1+k} + k\int_{\mathcal{T}} \left(1-(1-\rho_{\text{h}})F_{T'}(t-\text{T}_{\text{cad}})\right)\left(F_T(t)\right)^k f_T(t)\,\text{d}t, \end{aligned} \tag{C.8}$$

since $1/(1+k)$ is the probability that a given frame is the longest one in the timeslot. Assuming uniform transmission times, we get that

$$\begin{aligned} p_{\text{free}}(k) &= \frac{1}{1+k} + k\int_{\mathcal{T}} \left(1-(1-\rho_{\text{h}})\frac{t-\text{T}_{\text{cad}}-\text{T}_{\text{min}}}{t-\text{T}_{\text{min}}}\right)\left(\frac{t-\text{T}_{\text{min}}}{\Delta_T}\right)^k \frac{1}{\Delta_T}\,\text{d}t \\ &= \frac{1}{1+k} + \frac{k}{\Delta_T^{1+k}}\int_{\mathcal{T}} \left(1-(1-\rho_{\text{h}})\frac{t-\text{T}_{\text{cad}}-\text{T}_{\text{min}}}{t-\text{T}_{\text{min}}}\right)(t-\text{T}_{\text{min}})^k\,\text{d}t \\ &= 1 - \frac{1-\rho_{\text{h}}}{1+k}\left(c^{1+k} - (1+k)c + k\right), \end{aligned} \tag{C.9}$$

with $c = \text{T}_{\text{cad}}/\Delta_T$, and, therefore, the probability that the channel is sensed free is

$$\begin{aligned} p_{\text{free}} &= \sum_{k=0}^{\infty} \frac{(G_{\text{slot}})^k \text{e}^{-G_{\text{slot}}}}{k!} \cdot \left(1 - \frac{1-\rho_{\text{h}}}{1+k}\left(c^{1+k} - (1+k)c + k\right)\right) \\ &= \frac{1}{G_{\text{slot}}}\left(1 - \rho_{\text{h}}(1-G_{\text{slot}}) + (1-\rho_{\text{h}})(cG_{\text{slot}} - \text{e}^{-(1-c)G_{\text{slot}}})\right). \end{aligned} \tag{C.10}$$

Appendix D. Average duration of successfully sent frames

To evaluate the energy efficiency of the MAC schemes, we have to compute $\overline{N}_{\text{success}}$, the average number of bits in the payload of the frames that are successfully transmitted. This value can be estimated from $\overline{T}_{\text{success}}$, the average duration of the successfully transmitted frames, as follows. From (A.1), we obtain that the average number of symbols comprising the physical message of successful Lora frames is given by

$$\overline{N}_{\text{phy}} = \frac{\overline{T}_{\text{success}}}{\text{T}_{\text{sym}}} - \text{N}_{\text{preamble}} - 4.25. \tag{D.1}$$

Then, substituting this value in (A.2) and solving for $\text{N}_{\text{payload}}$, we get that $\overline{N}_{\text{success}}$ can be approximated as

$$\overline{N}_{\text{success}} \approx \left(\frac{\overline{T}_{\text{success}}}{\text{T}_{\text{sym}}} - \text{N}_{\text{preamble}} - 12.25\right)\cdot\text{CR}\cdot(\text{SF}-2\cdot\text{DE})+4\cdot\text{SF}-44. \tag{D.2}$$

In the following subsections we will compute $\overline{T}_{\text{success}}$ for each of the evaluated MAC schemes. Recall that, with S-ALOHA, the probability of success of frame transmissions does not depend on frame durations and, therefore, $\overline{T}_{\text{success}} = \overline{T}$.

D.1. P-ALOHA

With P-ALOHA, note that the longer the frame, the lower the probability of success of its transmission, since it is more likely that, during the transmission of a long frame, some other ED send a new frame. The probability density function of the duration of the frames successfully sent with P-ALOHA is $f_T(t)/p_2$, where p_2 is the probability that no ED starts a new transmission that collides with the ongoing transmission, as shown in (5). Therefore, the average duration of these frames can be computed as

$$\overline{T}_{\text{success}} = \frac{1}{p_2}\int_{\mathcal{T}} t\text{e}^{-tG/\overline{T}} f_T(t)\,\text{d}t. \tag{D.3}$$

Then, assuming uniform transmission times ($f_T(t) = 1/\Delta_T$), we get that

$$\begin{aligned} \overline{T}_{\text{success}} &= \frac{1}{p_2}\int_{\text{T}_{\text{min}}}^{\text{T}_{\text{max}}} t\text{e}^{-tG/\overline{T}}\frac{1}{\Delta_T}\,\text{d}t \\ &= \frac{(\text{T}_{\text{min}} + \overline{T}/G)\,\text{e}^{-G_{\text{min}}} - (\text{T}_{\text{max}} + \overline{T}/G)\,\text{e}^{-G_{\text{max}}}}{\text{e}^{-G_{\text{min}}} - \text{e}^{-G_{\text{max}}}}. \end{aligned} \tag{D.4}$$

D.2. CSMA

Similarly as done with P-ALOHA, the average duration of the frames successfully sent with CSMA can be computed as

$$\overline{T}_{\text{success}} = \frac{\text{e}^{\rho_{\text{h}}G_{\text{cad}}}}{p_2}\int_{\mathcal{T}} t\text{e}^{-t\rho_{\text{h}}G/\overline{T}} f_T(t)\,\text{d}t, \tag{D.5}$$

where p_2 is now the probability that no hidden ED starts a new transmission that collides with the ongoing transmission after the initial T_{cad} period, as shown in (8). Considering uniform transmission times as usual, we obtain

$$\begin{aligned} \overline{T}_{\text{success}} &= \frac{\text{e}^{\rho_{\text{h}}G_{\text{cad}}}}{p_2}\int_{\text{T}_{\text{min}}}^{\text{T}_{\text{max}}} t\text{e}^{-t\rho_{\text{h}}G/\overline{T}}\frac{1}{\Delta_T}\,\text{d}t \\ &= \frac{(\text{T}_{\text{min}} + \overline{T}/(\rho_{\text{h}}G))\,\text{e}^{-\rho_{\text{h}}G_{\text{min}}} - (\text{T}_{\text{max}} + \overline{T}/(\rho_{\text{h}}G))\,\text{e}^{-\rho_{\text{h}}G_{\text{max}}}}{\text{e}^{-\rho_{\text{h}}G_{\text{min}}} - \text{e}^{-\rho_{\text{h}}G_{\text{max}}}}. \end{aligned} \tag{D.6}$$

D.3. LFS-CSMA

Certainly, the frames successfully sent with our proposal are always the longest ones in each timeslot. As shown in Section 4.4, if there are $1+k$ frames waiting to be sent in a given timeslot, the probability density function of the duration of the longest one is $f_{T_{\text{long}}}(t) = (1+k)\left(F_T(t)\right)^k f_T(t)$, so the average duration of the longest frame in a timeslot with $1+k$ pending frames is

$$\overline{T}_{\text{long}}(k) = \int_{\mathcal{T}} t\,(1+k)\left(F_T(t)\right)^k f_T(t)\,\text{d}t. \tag{D.7}$$

Assuming uniform transmission times, we obtain that

$$\overline{T}_{\text{long}}(k) = (1+k)\int_{\text{T}_{\text{min}}}^{\text{T}_{\text{max}}} t\left(\frac{t-\text{T}_{\text{min}}}{\Delta_T}\right)^k \frac{1}{\Delta_T}\,\text{d}t = \frac{(1+k)\text{T}_{\text{max}} + \text{T}_{\text{min}}}{2+k}, \tag{D.8}$$

and, therefore, the average duration of the frames successfully sent is

$$\begin{aligned} \overline{T}_{\text{success}} &= \sum_{k=0}^{\infty} \frac{(G_{\text{slot}})^k \text{e}^{-G_{\text{slot}}}}{k!} \cdot \frac{(1+k)\,\text{T}_{\text{max}} + \text{T}_{\text{min}}}{2+k} \\ &= \frac{\text{e}^{-G_{\text{slot}}}}{G_{\text{slot}}^2}\left(\text{T}_{\text{min}}(1-(1-G_{\text{slot}})\text{e}^{G_{\text{slot}}}) + \text{T}_{\text{max}}(\text{e}^{G_{\text{slot}}}(G_{\text{slot}}^2 - G_{\text{slot}} + 1) - 1)\right). \end{aligned} \tag{D.9}$$

References

[1] J. Ploennigs, J. Cohn, A. Stanford-Clark, The future of IoT, IEEE Internet Things Mag. 1 (1) (2018) 28–33, http://dx.doi.org/10.1109/IOTM.2018.1700021.

[2] U. Raza, P. Kulkarni, M. Sooriyabandara, Low power wide area networks: an overview, IEEE Commun. Surv. Tutor. 19 (2) (2017) 855–873, http://dx.doi.org/10.1109/COMST.2017.2652320.

[3] W. Ayoub, A.E. Samhat, F. Nouvel, M. Mroue, J.-C. Prévotet, Internet of mobile things: overview of LoRaWAN, DASH7, and NB-IoT in LPWANs standards and supported mobility, IEEE Commun. Surv. Tutor. 21 (2) (2019) 1561–1581, http://dx.doi.org/10.1109/COMST.2018.2877382.

[4] LoRaWAN Specification v1.1, LoRa Alliance, 2017, URL https://lora-alliance.org/resource_hub/lorawan-specification-v1-1/.

[5] LoRa Alliance, 2022, URL https://lora-alliance.org/.

[6] T. Elshabrawy, J. Robert, Interleaved chirp spreading lora-based modulation, IEEE Internet Things J. 6 (2) (2019) 3855–3863, http://dx.doi.org/10.1109/JIOT.2019.2892294.

[7] F. Adelantado, X. Vilajosana, P. Tuset-Peiro, B. Martinez, J. Melia-Segui, T. Watteyne, Understanding the limits of LoRaWAN, IEEE Commun. Mag. 55 (9) (2017) 34–40, http://dx.doi.org/10.1109/MCOM.2017.1600613.

[8] T. Polonelli, D. Brunelli, A. Marzocchi, L. Benini, Slotted aloha on LoRaWAN - design, analysis, and deployment, Sensors 19 (4) (2019) http://dx.doi.org/10.3390/s19040838.

[9] M.O. Farooq, D. Pesch, A search into a suitable channel access control protocol for LoRa-based networks, in: 2018 IEEE 43rd Conference on Local Computer Networks, LCN, 2018, pp. 283–286, http://dx.doi.org/10.1109/LCN.2018.8638225.

[10] M. El-Aasser, R. Badawi, M. Ashour, T. Elshabrawy, Examining carrier sense multiple access to enhance LoRa IoT network performance for smart city applications, in: 2019 IEEE 9th International Conference on Consumer Electronics, ICCE-Berlin, 2019, pp. 168–173, http://dx.doi.org/10.1109/ICCE-Berlin47944.2019.8966182.

[11] M. Baddula, B. Ray, M. Chowdhury, Performance evaluation of aloha and CSMA for LoRaWAN network, in: 2020 IEEE Asia-Pacific Conference on Computer Science and Data Engineering, CSDE, 2020, pp. 1–6, http://dx.doi.org/10.1109/CSDE50874.2020.9411539.

[12] Y. Liu, L. Liu, J. Liang, J. Chai, X. Lei, H. Zhang, High-performance long range-based medium access control layer protocol, Electronics 9 (8) (2020) http://dx.doi.org/10.3390/electronics9081273.

[13] C. Pham, M. Ehsan, Dense deployment of LoRa networks: expectations and limits of channel activity detection and capture effect for radio channel access, Sensors 21 (3) (2021) http://dx.doi.org/10.3390/s21030825.

[14] A. Triantafyllou, P. Sarigiannidis, T. Lagkas, I.D. Moscholios, A. Sarigiannidis, Leveraging fairness in LoRaWAN: A novel scheduling scheme for collision avoidance, Comput. Netw. 186 (2021) http://dx.doi.org/10.1016/j.comnet.2020.107735.

[15] R. Piyare, A.L. Murphy, M. Magno, L. Benini, On-demand LoRa: asynchronous TDMA for energy efficient and low latency communication in IoT, Sensors 18 (11) (2018) http://dx.doi.org/10.3390/s18113718.

[16] B. Reynders, Q. Wang, P. Tuset-Peiro, X. Vilajosana, S. Pollin, Improving reliability and scalability of LoRaWANs through lightweight scheduling, IEEE Internet Things J. 5 (3) (2018) 1830–1842, http://dx.doi.org/10.1109/JIOT.2018.2815150.

[17] J. Haxhibeqiri, I. Moerman, J. Hoebeke, Low overhead scheduling of LoRa transmissions for improved scalability, IEEE Internet Things J. 6 (2) (2019) 3097–3109, http://dx.doi.org/10.1109/JIOT.2018.2878942.

[18] D. Zorbas, K. Abdelfadeel, P. Kotzanikolaou, D. Pesch, TS-LoRa: Time-slotted LoRaWAN for the industrial internet of things, Comput. Commun. 153 (2020) 1–10, http://dx.doi.org/10.1016/j.comcom.2020.01.056.

[19] D. Zorbas, X. Fafoutis, Time-slotted LoRa networks: design considerations, implementations, and perspectives, IEEE Internet Things Mag. 4 (1) (2021) 84–89, http://dx.doi.org/10.1109/IOTM.0001.2000072.

[20] D. Croce, M. Gucciardo, S. Mangione, G. Santaromita, I. Tinnirello, Impact of LoRa imperfect orthogonality: analysis of link-level performance, IEEE Commun. Lett. 22 (4) (2018) 796–799, http://dx.doi.org/10.1109/LCOMM.2018.2797057.

[21] S. Gao, X. Zhang, C. Du, Q. Ji, A multichannel low-power wide-area network with high-accuracy synchronization ability for machine vibration monitoring, IEEE Internet Things J. 6 (3) (2019) 5040–5047, http://dx.doi.org/10.1109/JIOT.2019.2895158.

[22] C. Pham, Investigating and experimenting CSMA channel access mechanisms for LoRa IoT networks, in: 2018 IEEE Wireless Communications and Networking Conference, WCNC, 2018, pp. 1–6, http://dx.doi.org/10.1109/WCNC.2018.8376997.

[23] J. Haxhibeqiri, F. Van den Abeele, I. Moerman, J. Hoebeke, LoRa scalability: a simulation model based on interference measurements, Sensors 17 (6) (2017) http://dx.doi.org/10.3390/s17061193.

[24] M. O'Kennedy, T. Niesler, R. Wolhuter, N. Mitton, Practical evaluation of carrier sensing for a LoRa wildlife monitoring network, in: IFIP Networking Conference, Paris, France, 2020.

[25] L. Beltramelli, A. Mahmood, P. Österberg, M. Gidlund, Lora beyond ALOHA: an investigation of alternative random access protocols, IEEE Trans. Ind. Informat. 17 (5) (2021) 3544–3554, http://dx.doi.org/10.1109/TII.2020.2977046.

Sergio Herrería-Alonso received the M.Sc. and Ph.D. degrees in telecommunication engineering from the University of Vigo, Spain, in 2001 and 2006, respectively, where he is currently an Associate Professor with the Department of Telematics Engineering, and an Affiliated Member of the co-located Networking Laboratory. He has authored or co-authored over 45 papers in peer-reviewed international conferences and journals, many of them with a high impact factor (Q1 and Q2 quartiles) in the WOS-Journal Citation Report. His main research interests include quality of service in the Internet, IoT technologies and networks, and energy-efficient networking.

Andrés Suárez-González received the Ph.D. in Telecommunications Engineering from the University of Vigo in 2000. Since 2001 he is an Associate Professor with the Department of Telematics Engineering, University of Vigo, where he is also an Affiliated Member of the co-located Networking Laboratory. He has published a book and co-authored over 64 conference and journal papers. His field of research has mostly been related to modeling and performance analysis of communication networks and traffic engineering.

Miguel Rodríguez-Pérez received the M.Sc. and Ph.D. degrees in telecommunication engineering from the University of Vigo, Spain, in 2001 and 2006, respectively. He is currently an Associate Professor with the Department of Telematics Engineering, University of Vigo, where he is also an Affiliated Member of the co-located Networking Laboratory. He has published a book and co-authored over 45 conference and journal papers. His research interests include congestion control and traffic engineering, with a strong focus on energy efficiency.

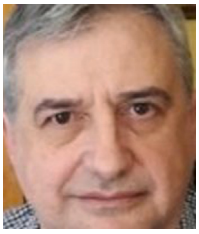

Cándido López-García received the M.Sc. and Ph.D. degrees in telecommunication engineering from the Universidad Politécnica de Madrid, Spain, in 1988 and 1995, respectively. He is currently a Full Professor with the Department of Telematics Engineering, University of Vigo, and an Affiliated Member of the co-located Networking Laboratory. He has authored or co-authored over 100 papers in international conferences and journals. His research interests include the area of performance evaluation in communication networks.